Measurement Principles of Optical Three-Axis Tactile Sensor and its Application to Robotic Fingers System

Hanafiah Yussof[1], Jumpei Takata[2] and Masahiro Ohka[3]
[1,3]Graduate School of Information Science, Nagoya University
[2]Olympus Corporation
[1]Faculty of Mechanical Engineering, Universiti Teknologi MARA
[1,2,3]Japan
[1]Malaysia

1. Introduction

A tactile sensor is a device that can measure a given property of an object or contact event through physical contact between the sensor and the object. Traditionally, tactile sensors have been developed using measurements of strain produced in sensing materials that are detected using physical quantities such as electric resistance and capacity, magnetic intensity, voltage and light intensity (Nicholls, 1990). Research on tactile sensor is basically motivated by the tactile sensing system of the human skin. In humans, the skin's structure provides a mechanism to simultaneously sense static and dynamic pressure with extremely high accuracy. Meanwhile in robotics, several tactile sensing principles are commonly used nowadays, such as capacitive, piezoelectrical, inductive, piezoresistive, and optoelectrical sensors (Schmidt et al., 2006, Lee & Nicholls, 1999).

In our research lab, with the purpose to establish object manipulation ability in robotic fingers, we developed a hemispherical shaped optical three-axis tactile sensor capable of acquiring normal and shearing forces to mount on the fingertips of robot fingers. This tactile sensor uses an optical waveguide transduction method and applies image processing techniques. Such a sensing principle is expected to provide better sensing accuracy to realize contact phenomena by acquiring the three axial directions of the forces, so that normal and shearing forces can be measured simultaneously. This tactile sensor is designed in a hemispherical dome shape that consists of an array of sensing elements. This shape is to mimics the structure of human fingertips for easy compliance with various shapes of objects. For miniaturization of the tactile sensor, measurement devices are placed outside the sensor. The small size of the sensor makes it easy for installation at robotic fingers.

The optical three-axis tactile sensor developed in this research is designed in hemispherical shape, and the sensing elements are distributed in 41-sub region. Due to this structure, the acquired images by CCD camera, except for sensing element at the sensor tip area, are not the actual image of contact pressure at the sensing elements. Therefore, to compensate with the sensor structure, it is necessary to conduct coordinate transformation calculations for each sensing element except for the element at the sensor tip area. In this chapter, we

present calculations to define coordinate transformation of the sensing elements on the sensor's hemispherical shape dome. Meanwhile, in the tactile sensor controller, since the image was warped due to projection from a hemispherical surface, image processing software Cosmos32 installed in the computer modifies the warped image data based on the coordinate transformation formulations, and calculates the integrated gray-scale value and displacement of gray-scale distribution to obtain the applied three-axis forces at the sensing element. Finally, we conduct experiment to evaluate the performance of the optical three-axis tactile sensor system using 3-dofs robotic fingers. We analyze the performance of tactile sensing feedback on the robot finger system to define optimum grasp pressure on the object surface. Figure 1 shows the robotic fingers mounted with the optical three-axis tactile sensors on each of its fingertips.
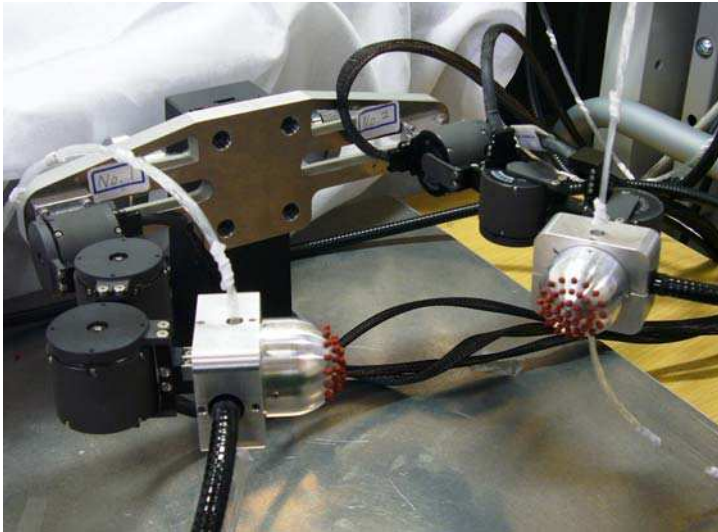

Fig. 1. Robotic fingers with optical three-axis tactile sensor.

2. Motivations and current state-of-the-art survey

The sense of touch is one of the five main sensing modalities in humans besides sight, sound, smell, and taste. It will play an important role in robotic paradigms toward effective manipulation and collaboration with humans in built-for-human environments. Research on tactile sensor is basically motivated by tactile sensing system of human skin. In daily life, humans regularly apply tactile sensing to support motions and perform tasks. However, in a developmental robot, tactile sensors are especially appropriate sensing devices that have too often been neglected in favor of vision-based approaches.

To date, while much research has developed visual and auditory sensors, comparatively little progress has been made on sensors that translate the sense of touch. This apparent neglect reflects the complexity of tactile sensing itself, because tactile sensing through the skin is not a simple transduction of one physical property into electronic signals. Furthermore tactile sensing is difficult to imitate, unlike sight and sound, which are well-defined physical quantities. In addition, the fact that a tactile signal is distributed over a

Measurement Principles of Optical Three-Axis Tactile Sensor and
its Application to Robotic Fingers System
125

much wider area and lacks such localized sensory organs as eyes and ears complicates the developmental of artificial sensory devices.

Nonetheless, realizing that the development of intelligent tactile sensors will help advance the evolution of human and robots working together in real life is encouraging (Ohmura et al., 2006, Kuniyoshi et al., 2004, Natale & Torres-Jara, 2006, Ohmura & Kuniyoshi, 2007). Indeed, researchers have recently agreed that a tactile sensor system is an essential sensory device to support the robot control system, particularly for object manipulation tasks (Omata et al., 2004, Kerpa et al., 2003, Lee & Nicholls, 1999). This agreement reflects the tactile sensor's capability to simultaneously sense normal force, shearing force, and slippage, thus offering exciting possibilities for determining object shape, texture, and property.

To date, several basic sensing principles are commonly in use in tactile sensor, such as capacitive sensor, piezoelectrical sensor, inductive sensor, optoelectrical sensor and piezoresistive sensor (Lee & Nicholls, 1999). In this research, with the aim of establishing object manipulation ability in real humanoid robot, we have developed an optical three-axis tactile sensor using optical waveguide transduction method, applying image processing techniques. This type of sensing principle is comparatively provides better sensing accuracy to detect contact phenomena from acquisition of three axial directions of forces, thus normal force and shearing force can be measured simultaneously (Ohka et al., 2004, Hanafiah et al. 2006, Hanafiah et al. 2007). The proposed three-axis tactile sensor has high potential compared to ordinal tactile sensor for fitting to a dextrose robotic arm to perform robot manipulation tasks.

3. Hardware structure

The optical three-axis tactile sensor developed in this research is designed in a hemispherical dome shape that consists of an array of sensing elements. This shape is to mimics the structure of human fingertips for easy compliance with various shapes of objects. For miniaturization of the tactile sensor, measurement devices are placed outside the sensor. The small size of the sensor makes it easy for installation at the robotic fingers.

The hardware novelty is shown in Fig. 2. It consists of an acrylic hemispherical dome, an array of 41 pieces of sensing elements made from silicon rubber, a light source, an optical fiber-scope, and a CCD camera. The optical fiber-scope is connected to the CCD camera to acquire image of sensing elements touching acrylic dome inside the tactile sensor. At this moment, light emitted from the light source is directed toward the edge of the hemispherical acrylic dome through optical fibers. A total of 24 pieces optical fibers are used; 12 pieces each at left and right side of the sensor, transmitting halogen light from the light source. The light directed into the acrylic dome remains within it due to total internal reflection generated, since the acrylic dome is surrounded by air having a lower reflection index than the acrylic dome. This make the acquired image by the CCD camera become clear even the sensor is hemispherical shape.

Meanwhile, the silicone rubber sensing element is comprised of one columnar feeler and eight conical feelers which remain in contact with the acrylic surface while the tip of the columnar feeler touches an object. The sensing elements are arranged on the hemispherical acrylic dome in a concentric configuration with 41 sub-regions. Such orientation is expected to provide good indication of contact pressure during performing object manipulation.
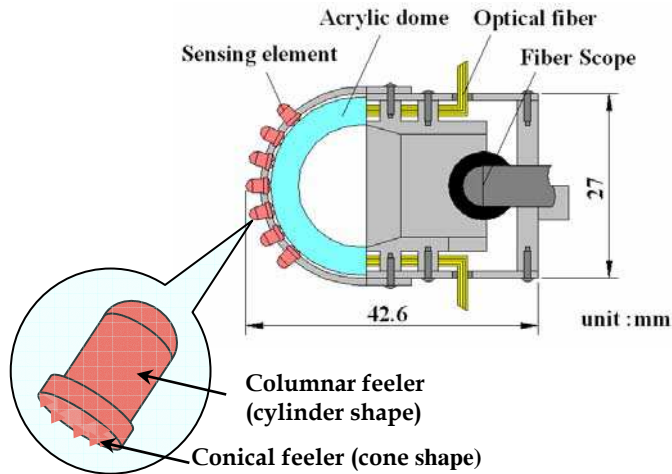
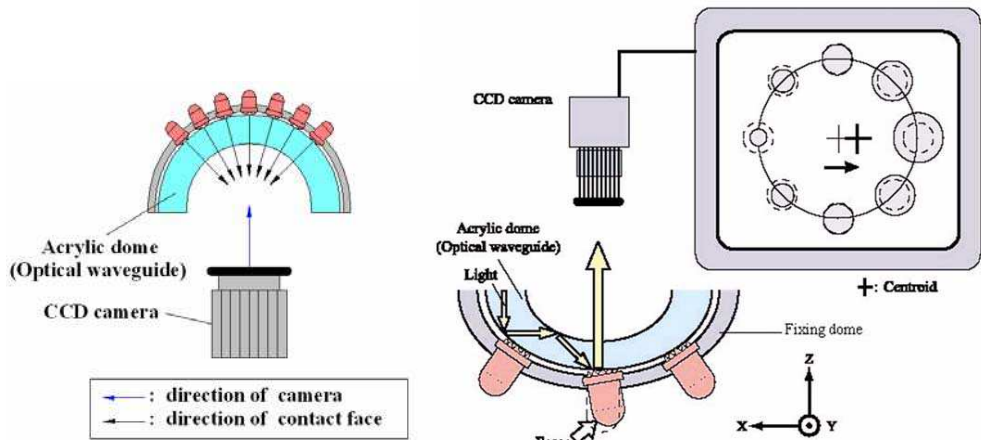Fig. 2. Structure of hemispherical dome shaped optical three-axis tactile sensor.

Fig. 3. Sensing principle of optical three-axis tactile sensor system.

4. Sensing principles

The optical three-axis tactile sensor is based on the principle of an optical waveguide-type tactile sensor. Figure 3 shows the sensing principle of the optical three-axis tactile sensor system. The light emitted from the light source is directed towards the edge of the hemispherical acrylic dome through optical fibers. When an object contacts the columnar feelers, resulting in contact pressure, the feelers collapse. At the points where the conical feelers collapse, light is diffusely reflected out of the reverse surface of the acrylic surface because the rubber has a higher reflective index. Contact phenomena consisting of bright spots caused by the collapse of the feelers are observed as image data, which are retrieved by the optical fiber-scope connected to the CCD camera and transmitted to the computer.

Figure 4 shows the real image data of contact phenomenon inside the tactile sensor acquired by the CCD camera where some bright area resulted from contact pressure can be observed at the sensing elements. Referring to Fig. 3, for normal force detection, when load is applied vertically to sensing elements, the conical feelers will collapse on acrylic dome surface. At this moment, the image retrieved by CCD camera shows brightness change at the area where conical feelers are collapse. The normal force is calculated based on the brightness of this area. At this moment, centroid point of the sensing element is remaining unchanged. Meanwhile, in shearing force detection, when tangential force is applied to the sensing element, the sensing element is collapse according to the applied load direction. In the same time, the centroid point of the sensing element also shifted. Therefore, the shearing force can be calculated based on horizontal displacement of this centroid point.

The system conception of the optical three-axis tactile sensor system is shown in Fig. 5. As explained previously, when contact pressure is applied on the tactile sensor elements, a bright spot areas are appeared inside the tactile sensor which then captured as image data by a CCD camera. The image data retrieved by the CCD camera are delivered to PC via PCI bus of image processing board Himawari PCI/S. Then the image data are saved in an internal buffer area that created inside the PC internal memory space.
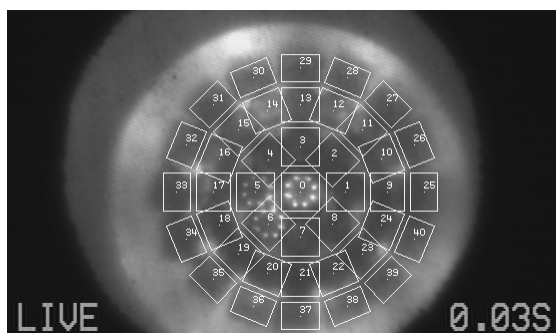
Contact phenomenon and 41 sub-regions of sensor elements inside the optical three-axis tactile sensor

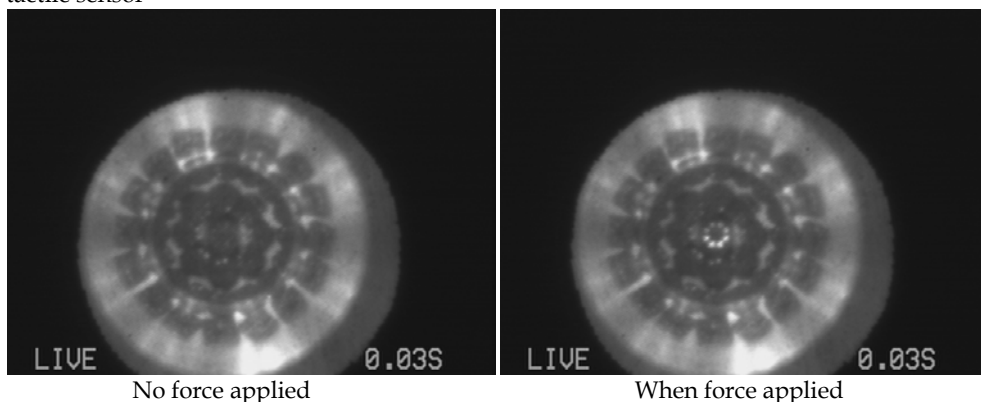No force applied   When force applied

Fig. 4. CCD camera images of contact phenomenon in the hemispherical shaped optical three-axis tactile sensor.

The image capture cycle was initially fixed at 1/30 seconds. Sensing program inside the PC is using Visual C++ and we utilized image analysis software Cosmos32 to analyze and measure the image data. During measurement process, the dividing procedure, digital filtering, integrated gray-scale value and centroid displacement are controlled on the PC using sensing program which created based on the software Cosmos32 functions.

Figure 6 shows system conception diagram of the sensing program which consists of image analysis module and connection module. This sensing program embedded a user interface and a tactile information structure which designed for both modules to share the tactile sensing data. The image analysis module uploads the image data from internal buffer and performs image analysis and measurement to define forces that applied to the sensing elements and also centroid point displacement. The upload cycle was fixed by the operator so that it not less than the image captured cycle.
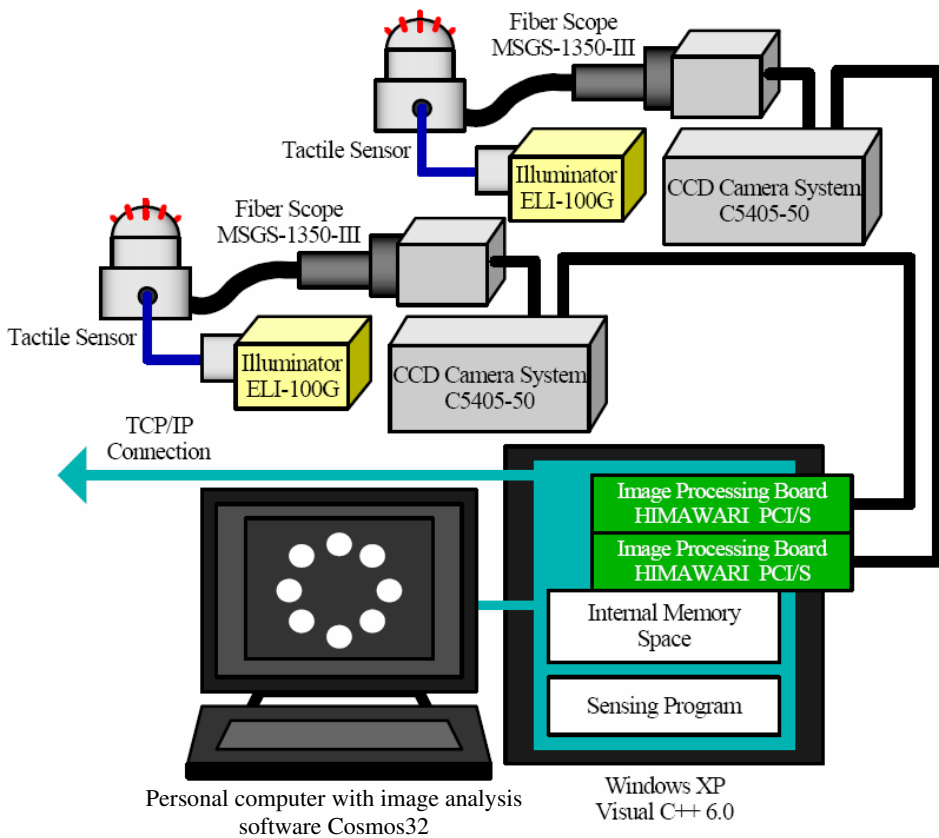

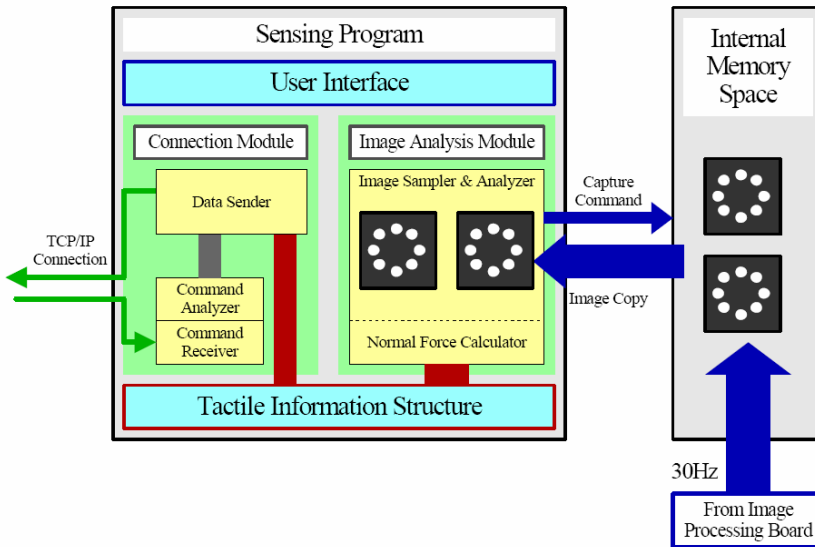Fig. 5. System conception diagram of tactile sensor system.

Measurement Principles of Optical Three-Axis Tactile Sensor and
its Application to Robotic Fingers System
129

Fig. 6. System conception of sensing program.

5. Measurement principles

In measurement process, the normal force of the F_x, F_y and F_z values are calculated using integrated gray-scale value G, while shearing force is based on horizontal centre point displacement. The displacement of gray-scale distribution u is defined in (1), where i and j are the orthogonal base vectors of the x- and y-axes of a Cartesian coordinate, respectively. This equation is based on calibration experiments, and material functions are identified with piecewise approximate curves (Ohka et al. 2006, Takata, 2005). Consequently, each force component is defined in (2).

$$u = u_x i + u_y j \tag{1}$$

$$F_x = f(u_x),\ F_y = f(u_y),\ F_z = g(G) \tag{2}$$

The optical three-axis tactile sensor developed in this research is designed in hemispherical shape, and the sensing elements are distributed in 41-sub region. Due to this structure, the acquired images by CCD camera, except for sensing element at the sensor tip area, are not the actual image of contact pressure at the sensing elements. Therefore, to compensate with the sensor structure, it is necessary to conduct coordinate transformation calculations for each sensing element except for the element at the sensor tip area.

5.1 Calculation of contact pressure and centroid position

As explained in previous section, when force is applied to columnar feeler of the tactile sensor element, the conical feeler collapsed on the acryl dome surface which created a bright spot retrieved by the CCD camera. To measure the applied forces, we measure the integrated gray-scale value of the bright area and also centroid point displacement.

According to current research (Ohka et al, 2006), integrated gray-scale value of the contact area $g(x,y)$ is proportional with contact force $p(x,y)$, as shown in (3).

$$p(x,y) = C_v \Delta g(x,y) \tag{3}$$

Here, C_v is a transformation coefficient, $\Delta g(x,y)$ is increment of the integrated gray-scale value. According to this relationship, we define normal force from gray-scale distribution of the contact area. Measurement of contact force P is defined from the following integration, where S is size of the gray-scale measurement area.

$$P = \int_S p(x,y) dS \tag{4}$$

Here, when equation (3) is applied to equation (4), we can define measurement of contact force P as following equation (5).

$$P = C_v \int_S \Delta g(x,y) dS \tag{5}$$

Next, we calculate the centroid position. The centroid position is measured according to center point of the bright spots area, which equal to center position of integrated gray-scale measurement area. When tangential force is applied to the sensor element, contact area of conical feeler at the sensor element with acryl surface is shifted horizontally. To define shearing force, we measure the horizontal centroid point displacement at x and y axes. At first, by applying the increment of integrated gray-scale value $\Delta g(x,y)$, the centroid positions at xy-axes which described at as x_G and y_G are define within the measurement area of integrated gray-scale value as shown in (6) and (7), respectively.

$$x_G = \frac{\int_S \Delta g(x,y) x dS}{\int_S \Delta g(x,y) y dS} \tag{6}$$

$$y_G = \frac{\int_S \Delta g(x,y) y dS}{\int_S \Delta g(x,y) x dS} \tag{7}$$

According to the above equations, displacement of centroid point at x y-axes in time t are defined as following equations.

$$dx_G^{(t)} = x_G^{(t)} - x_G^{(t-1)} \tag{8}$$

$$dy_G^{(t)} = y_G^{(t)} - y_G^{(t-1)} \tag{9}$$

5.2 Coordinate transformation on hemispherical shaped dome

The optical three-axis tactile sensor developed in this research is designed in hemispherical shape, and the sensing elements are distributed in 41-sub region as shown in Fig. 4. Due to this structure, the acquired images by CCD camera, except for sensing element at the sensor tip area #0, are not the actual image of contact pressure at the sensing elements. Therefore,

to compensate with the sensor structure, it is necessary to conduct coordinate transformation calculation for each sensing element except for element #0.
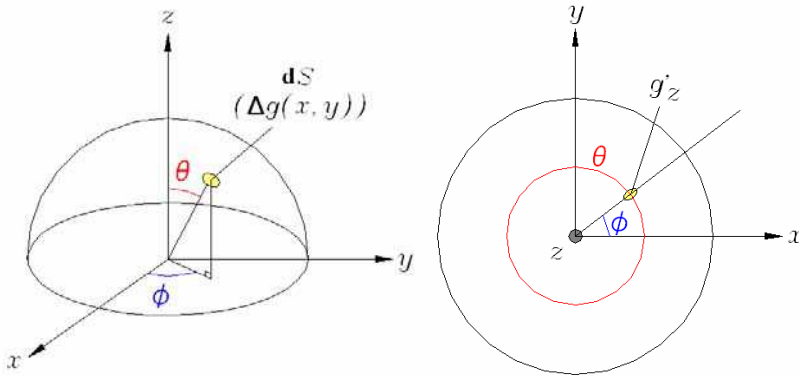

Fig. 7. Diagram of hemispherical dome indicates measurement area of integrated gray-scale value for coordinate transformation calculation.

Referring to Fig. 7, where *dS* is a measurement area of integrated gray-scale value, coordinate transformation is described in equation (10). Here (g_x, g_y, g_z) is integrated gray-scale value before coordinate transformation, meanwhile (g'_x, g'_y, g'_z) is after the transformation.

$$\begin{bmatrix} g'_x \\ g'_y \\ g'_z \end{bmatrix} = \begin{bmatrix} \cos\theta\cos\phi & -\sin\phi & \sin\theta\cos\phi \\ \cos\theta\sin\phi & \cos\phi & \sin\theta\sin\phi \\ -\sin\theta & 0 & \cos\theta \end{bmatrix} \begin{bmatrix} g_x \\ g_y \\ g_z \end{bmatrix} \tag{10}$$

If *dS* is put on the sensor tip area, equation (10) is become like equation (11), where the increment of the integrated gray-scale value can be described as $\Delta g(x,y) = g_z(x,y)$.

$$\begin{bmatrix} g'_x \\ g'_y \\ g'_z \end{bmatrix} = \begin{bmatrix} \cos\theta\cos\phi & -\sin\phi & \sin\theta\cos\phi \\ \cos\theta\sin\phi & \cos\phi & \sin\theta\sin\phi \\ -\sin\theta & 0 & \cos\theta \end{bmatrix} \begin{bmatrix} 0 \\ 0 \\ g_z \end{bmatrix} \tag{11}$$

Here, equation (11) is solved as following equations:

$$g'_x = g_z \sin\theta\cos\phi \tag{12}$$

$$g'_y = g_z \sin\theta\sin\phi \tag{13}$$

$$g'_z = g_z \cos\theta \tag{14}$$

Hence, when measurement area of integrated gray-scale value is put on the sensor tip area, the integrated gray-scale value after coordinate transformation is coincide with $g_z(x,y)$ as shown in the following equation.

$$g'_x \sqrt{g'_x + g'_y + g'_z} = g_z \sqrt{\sin^2 \theta \cos^2 \phi + \sin^2 \theta \sin^2 \phi + \cos^2 \theta}$$

$$= g_z \sqrt{\sin^2 \theta + \cos^2 \theta} \qquad (15)$$

$$= g_z$$

Here, from (14), the increment of the integrated gray-scale value is define as follows:

$$\Delta g(x, y) = \frac{g_z}{\cos \theta} \qquad (16)$$

From equation (16), the coordinate transformation for measurement of contact force P from equation (5) is described as follows:

$$P = C_v \int_S \Delta g(x, y) dS$$
$$= C_v \int_S \frac{g'_z}{\cos \theta} dS \qquad (17)$$

Consequently, the captured image by CCD camera for measurement area dS' on the hemispherical dome is corrected to measurement area dS by defining integrated gray-scale value g'_z using equation (17).

6. Application in robotic fingers system

The hemispherical shaped optical three-axis tactile sensors are mounted on fingertips of robotic finger. The robotic finger system is comprised of two articulated fingers, each of which has 3-dofs with micro-actuators that are used in each joint. This system is comprised of two main controllers: finger controller and tactile sensor controller. Each of these controllers is connected to each other using TCP/IP protocols via the internet.

6.1 Finger controller
The control system architecture of the robot finger controller, which is based on tactile sensing, is shown in Fig. 8. This controller is comprised of three modules: connection module, thinking routines, and hand/finger control module. It is connected with tactile sensor controller by the connection module using TCP/IP protocols (Takata, 2005, Hanafiah et al., 2008). The most important considerations in controlling finger motions during performing object manipulation tasks are: what kind of information are acquired from the tactile sensor, how to translate and utilize this information, and how to send command to robot finger so that velocity of the finger motion can be control properly. These processes are performed inside the thinking routines module.
As shown in Fig. 8, inside the thinking routines module, there is thinking routine chooser consists of pin status analyzer and velocity generator. Moreover, there is motion information structure which connecting to both pin status analyzer and velocity generator. The pin status analyzer module is functioned to receive information from the tactile sensor about sensing elements condition, and use this information to decide suitable motion mode. Then

it sends to the connection module a list of sensing elements that acquire tactile sensing information. Meanwhile, the velocity generator module is functioned to decide finger velocity based on finger information structure and motion information structure. The motion information structure consists of initial velocity, motion flag mode, etc, which is used to control finger movement. Meanwhile, finger information structure provides connection all modules so that they can share data of finger orientation, joint angle and tactile sensing data from each sensor elements.
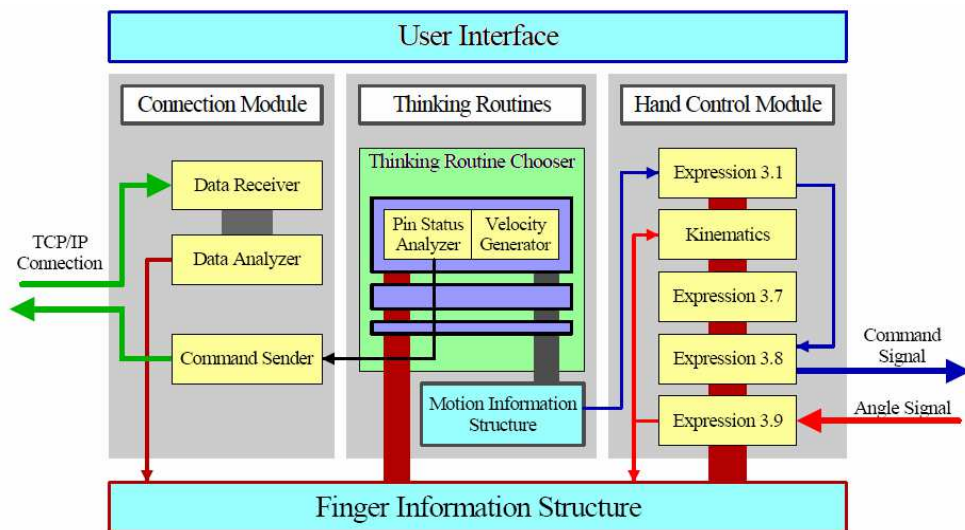

Fig. 8. Control system structure of robotic fingers.

User Interface was designed for the operator to provide commands to the finger control system. Finger control module controls the finger motion by calculating joints velocity and angle. In fact, this module can move finger without using sensing feedback. Thinking routines module receives tactile sensing data from tactile sensor and uses it to calculate fingertip velocity. In addition, to obtain low force interactions of the fingers during exploring object surface without causing damage, rotation velocity at each joint is defined precisely based on joint angle obtained in kinematics calculations, whereby force-position controls are performed.

6.2 Sensor controller

Figure 9 shows layout of tactile sensor controller. In the tactile sensor controller, based on image data captured by CCD camera, an image processing board Himawari PCI/S (Library Corp.) function as PCI bus picks up the image and sends it to internal buffer created inside the PC main memory. Sampling time for this process is 1/30 seconds. We use PC with Windows XP OS installed with Microsoft Visual C++. The image data are then sent to image analysis module applying Cosmos32 software which controls the dividing procedure, digital filtering, calculation of integrated gray-scale value and centroid displacement.

Since the image warps due to projection from a hemispherical surface as shown in Fig. 2, the software Cosmos32 with auto image analysis program installed in the computer modifies

the warped image data and calculates G, u_x and u_y to obtain the three-axis force applied to the tip of the sensing element using equation (2). These control schemes enable the finger controller to perform force-position control to adjust grasp pressure of the two fingers.
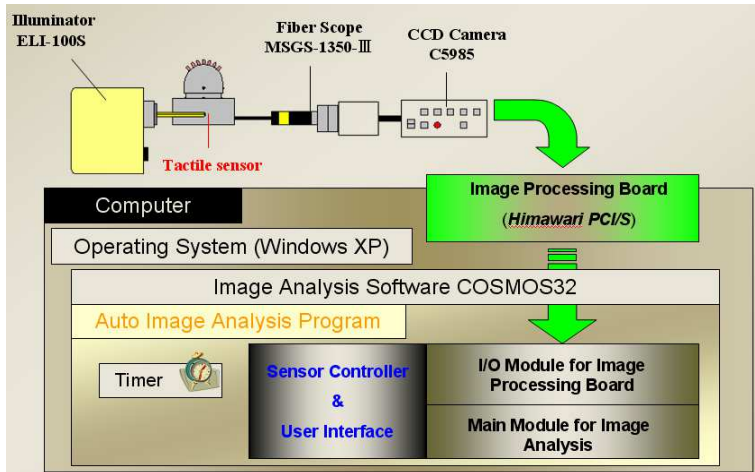

Fig. 9. Control system structure of optical three-axis tactile sensor.

6.3 Control algorithm

To further understand about data communication process in the finger controller, we present a simple case study where finger touches an object and then avoid/evade the object by moving the finger to reverse direction. At first, the finger moving velocity to search for object is defined as V_0. Next, we fix thresholds of normal force F_1 and F_2. During searching process, when any of sensor elements touch an object, and if the detected normal force F_n is exceeding normal force threshold F_1 [N], the finger will stop moving. Meanwhile, if the detected normal force F_n is exceeding threshold F_2 [N], the finger will move towards reverse direction of the sensing element that detects the highest force. At this moment the reverse velocity is defined as $|V_{re}|$. The parameters values of V_0, F_1, F_2 and $|V_{re}|$ are saved inside the motion information structure. The thresholds F_1 and F_2 are also delivered to sensor controller. When finger start moving, command to request status of each sensor elements are delivered to the sensor system according to control sampling phase of the finger system. Detail of data communication process for the pin status analyzer is shown in Fig. 10.

The processes at the pin status analyzer are explained as follows:

1. When sensor system received request command pin status analyzer, it will feedback status flag of each requested sensing element condition.
2. Connection module received the feedback data and then sends this data to the pin status analyzer, as well keeps it inside the finger information structure.
3. Pin status analyzer will then reset the finger motion ("STOP" and "EVADE") inside the motion information structure.
4. If the pin status analyzer received data flag that exceeds F_1 or F_2, or both of them, it will list up the concerned sensor elements. The pin status analyzer will rise up "STOP" flag if any listed sensor element is exceeded F_1, meanwhile it will rise-up "EVADE" flag if any listed sensor element is exceeded F_2. Then it sent the lists of data to the connection module.

5. The connection module will create a command to request normal force data of related sensor elements, and send the request to sensor system.
6. When sensor system received this request command, it will feedback normal force data of the requested sensor element to connection module at the finger controller.
7. Connection module received the feedback normal force data and then sends it to finger information structure. Based on this data, the velocity generator module will decide the velocity of the finger.
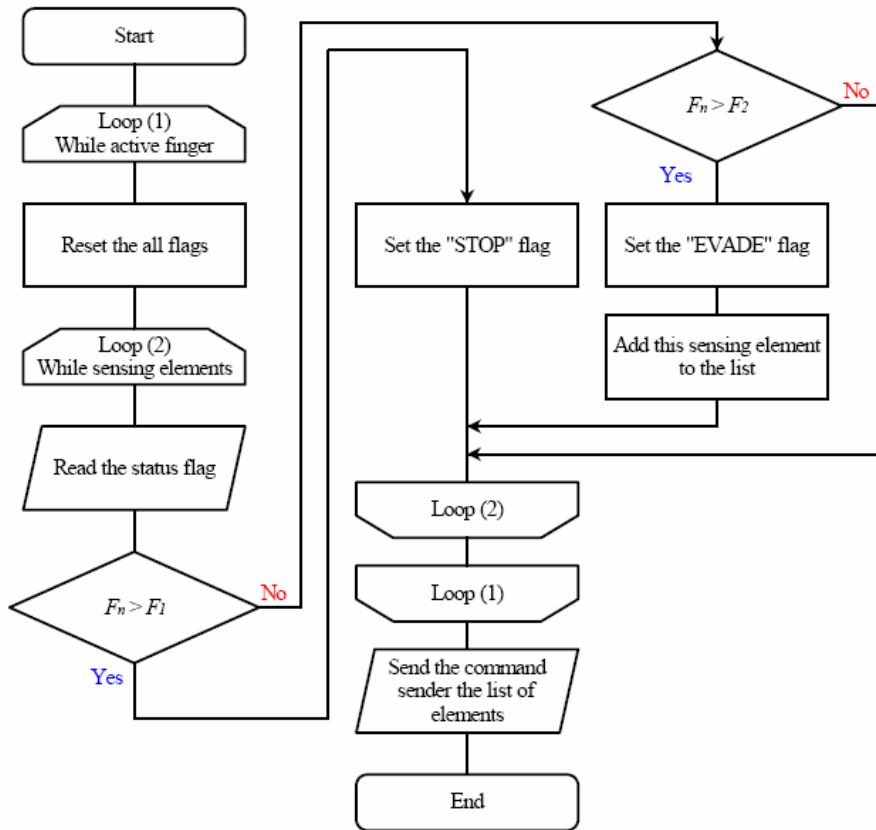

Fig. 10. Example of flowchart at the pin status analyzer for case study.

Figure 11 shows flowchart at the motion generator for case study. The processes are explained as follows:

1. If no flags "STOP" or "EVADE" rise-up, finger will move according to initial velocity V_0.
2. If "STOP" flag is rise-up, finger velocity becomes 0.
3. If "EVADE" flag is rise-up, the finger will move towards reverse direction of the sensing element that detects the highest normal force value. To decide the finger velocity, when finger evading velocity is described as $V_r = (V_{rx}, V_{ry}, V_{rz})$, the direction cosine in the frame of workspace $(\alpha_{Gk}, \beta_{Gk}, \gamma_{Gk})$ is calculated as equation (18).

$$V_r = -|V_{re}| \begin{bmatrix} \alpha_{Gk} \\ \beta_{Gk} \\ \gamma_{Gk} \end{bmatrix} \tag{18}$$

Here, basically this generation of velocity is sent to hand/finger control module to solve the joint rotation velocity at the finger derived by kinematics-based Resolved Motion Rate Control (RMRC), which commonly known as an algorithm for solving path-tracking problem in robotic control (Umetani & Yoshida, 1989). Therefore, controls of the finger based on tactile sensing information are conducted.
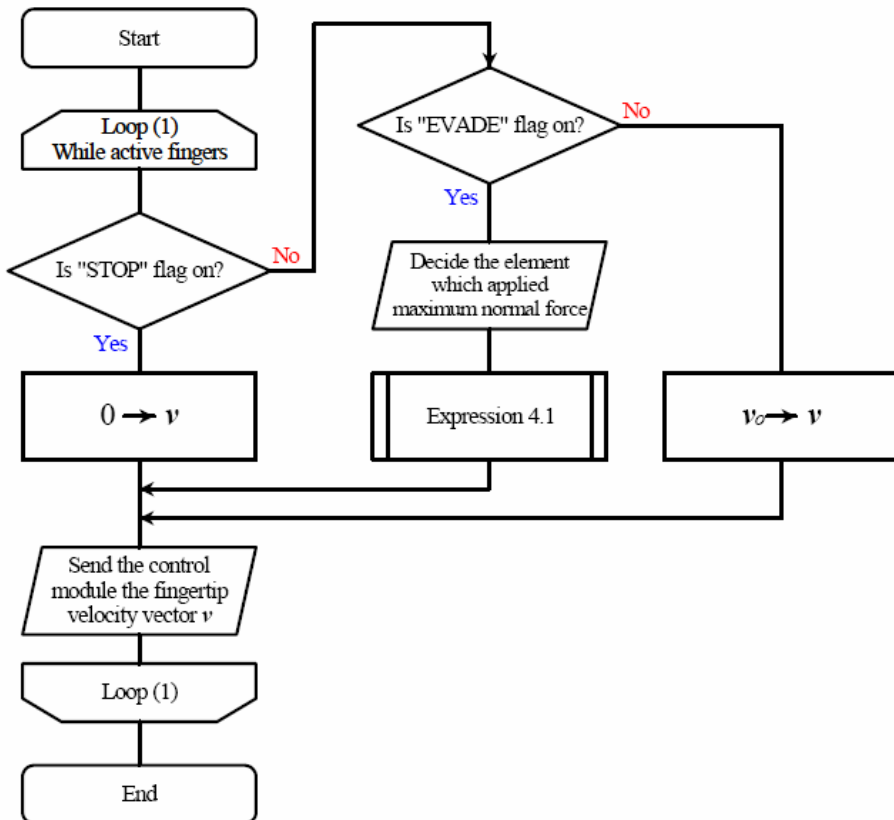

Fig. 11. Example of flowchart at the motion generator for case study.

7. Performance evaluation

We conduct object manipulation experiment using the robotic fingers system. We used a wood block as an object. In this experiment, at first the two fingers grasp the object to define optimum gripping pressure. At this moment, the grasp pressure is controlled by parameters of normal force thresholds. Then both fingers lift up the object to *z*-axis direction while

maintaining the optimum grasp pressure. During this motion, both normal pressure and slippage are concerned. Therefore the finger controller utilized parameters of normal force and centroid change thresholds. Here, when shearing force exceeds the centroid change threshold, the finger's velocity for reinforcing the grasping pressure is calculated using equation (19), whereby vector velocity of the finger $v+\Delta v$ is defined by finger control module in the finger controller.

$$\Delta v = \left| v_p \right| \begin{bmatrix} \alpha_{Gk} \\ \beta_{Gk} \\ \gamma_{Gk} \end{bmatrix} \tag{19}$$

Table 1 shows control parameters in the robotic fingers system. These parameters value was determined from calibration experiments conducted using soft and hard objects (Hanafiah et al. 2008). Figure 12 shows photographs of the robot arm performing object manipulation with wood block. In this experiment, both fingers move along x-axis direction to grasp the wood block. When optimum grasping pressure is defined and the robot recognized the hardness of the object, both fingers lift up the wood block along y-axis, and then move forward along z-axis. Figure 13 shows relation between normal force and fingertip movement at x-, y- and z-axes for left finger. Accordingly, Fig. 14 shows relation between amount of x-directional centroid change and fingertip movement at x-, y-, and z-axes for left finger.

From these graphs, we can observe that the tactile sensor managed to detect normal and shearing forces applied to the sensing elements during manipulating object. Finger controller used this information to control grasp pressure against the object. The fingers movement stopped when the detected normal force reached to threshold F_1. Meanwhile, threshold of centroid change is used to control re-push velocity of the fingers when slippage occurred during grasping.

Category		Parameter
Sampling interval	Sensor	100 ms
	Finger	25 ms
Threshold of normal force	F_1	0.5 N
	F_2	1.8 N
Threshold of centroid change	dr	0.004 mm
Velocity of re-push	v_p	2 mm/s
Progress time	Δt	0.1 s

Table 1. Control parameters in robotic fingers system.

This experimental result shows that the fingers managed to grasp the objects within optimum grasp pressure, lift it to upwards direction, and then performed some movements manipulating the objects. The experimental results also revealed that the robotic fingers system mounted with the hemispherical shaped optical three-axis tactile sensor managed to grasp the object within optimum grasp pressure without causing damage to the object and the sensor elements. In addition, the formulations applied in this system enabled precise control of the fingertips from determination of joint rotation angles and velocity.
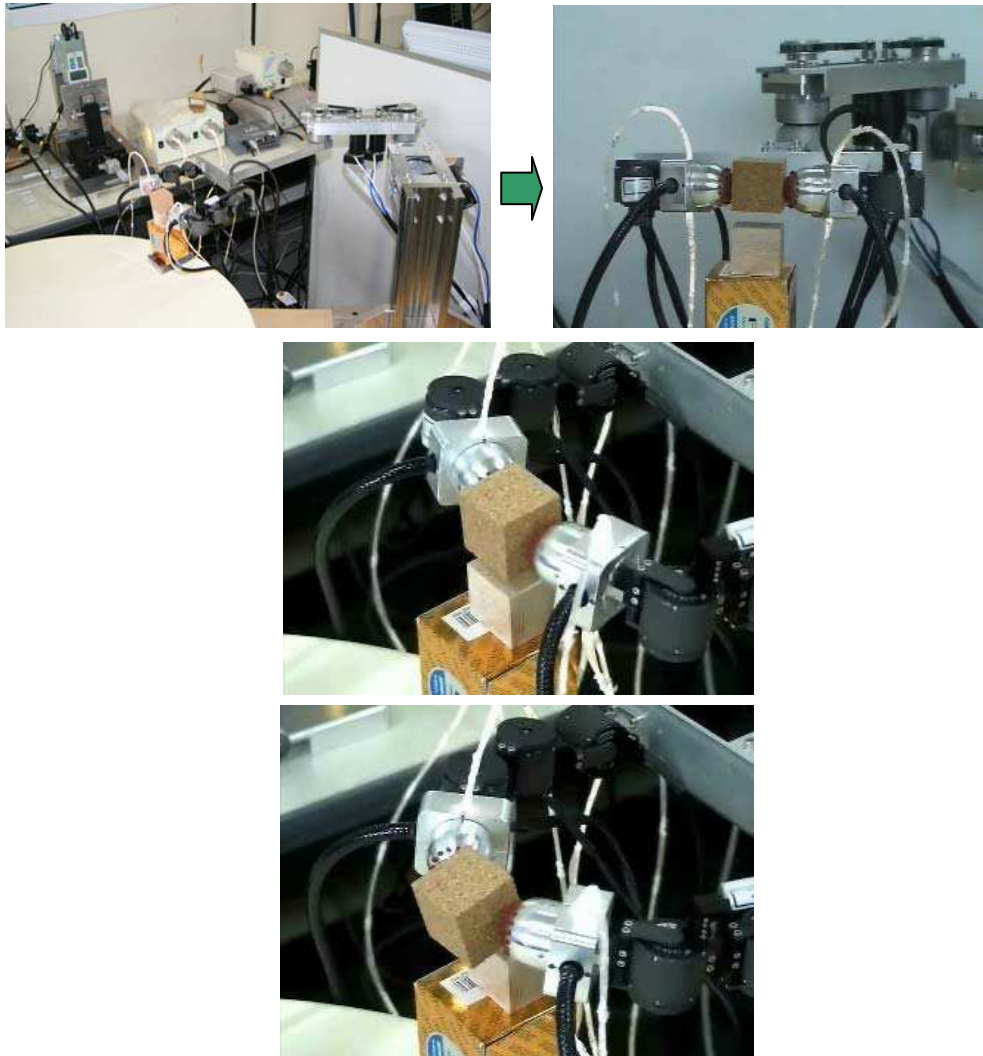
Fig. 12. Experiments of two robotic fingers manipulate wood block.
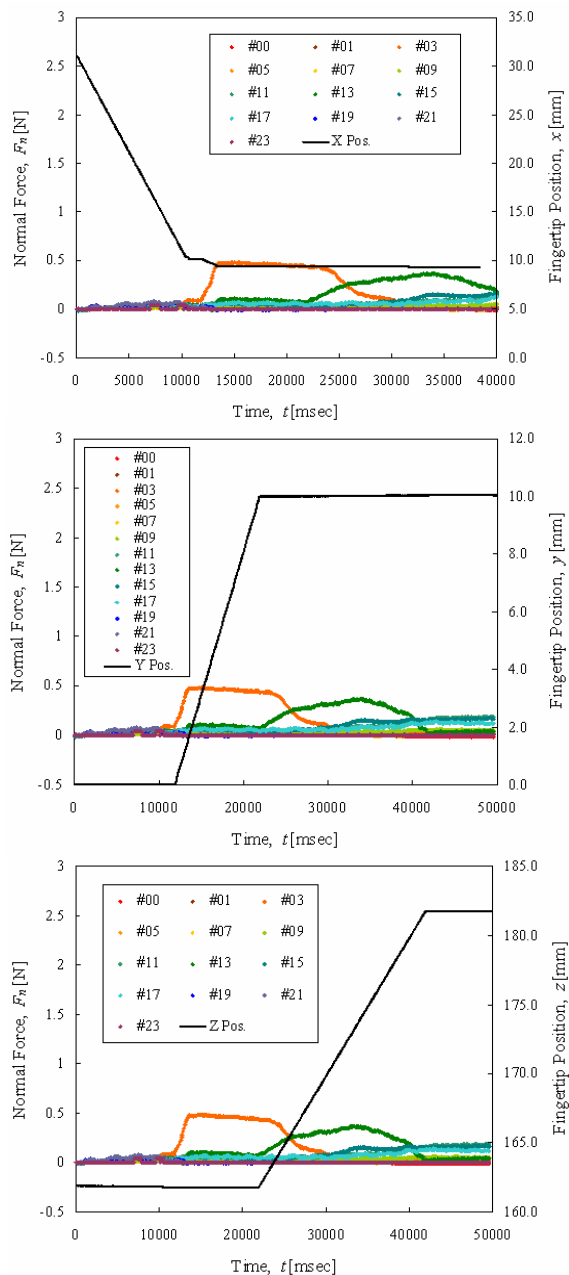
Fig. 13. Experiments of two robotic fingers manipulate wood block; data for left finger: *(Top)* Relation between normal force and fingertip movement at *x*-axis. *(Middle)* Relation between normal force and fingertip movement at *y*-axis. *(Bottom)* Relation between normal force and fingertip movement at *z*-axis.
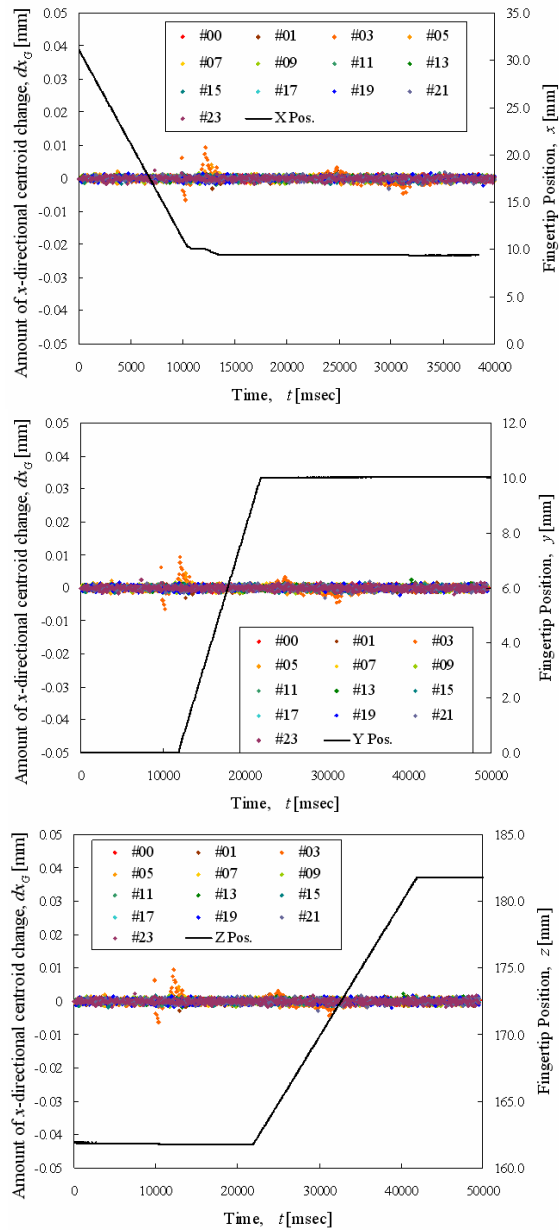
Fig. 14. Experiments of two robotic fingers manipulate wood block; data for left finger: *(Top)* Relation between amount of x-directional centroid change and fingertip movement at *x*-axis. *(Middle)* Relation between amount of x-directional centroid change and fingertip movement at *y*-axis. *(Bottom)* Relation between amount of x-directional centroid change and fingertip movement at *z*-axis.

Measurement Principles of Optical Three-Axis Tactile Sensor and
its Application to Robotic Fingers System
141

8. Conclusion

In this research we developed the original hemispherical shaped optical three-axis tactile sensor system to mount on robotic fingers. The tactile sensor is capable of acquiring normal and shearing forces, which are the most important sensing elements in object manipulation tasks. This tactile sensor is designed in a hemispherical dome shape that consists of an array of sensing elements. This shape is to mimics the structure of human fingertips for easy compliance with various shapes of objects. This tactile sensor uses an optical waveguide transduction method and applies image processing techniques. Such a sensing principle is expected to provide better sensing accuracy to realize contact phenomena by acquiring the three axial directions of the forces, so that normal and shearing forces can be measured simultaneously.

In this chapter, we have presented force detection and measurement principles of the tactile sensor for normal and shearing forces. The normal force is calculated based on brightness changes of visual image taken by CCD camera. To define the applied force, we measure the integrated gray-scale value of the bright area. Meanwhile, shearing force is calculated by measuring centroid point displacement of the bright area retrieved by the CCD camera.

The optical three-axis tactile sensor developed in this research is designed in hemispherical shape, and the sensing elements are distributed in 41-sub region. Due to this structure, the acquired images by CCD camera, except for sensing element at the sensor tip area, are not the actual image of contact pressure at the sensing elements. Therefore, to compensate with the sensor structure, we conducted calculations to define coordinate transformation of the sensing elements on the sensor's hemispherical shape dome.

The optical three-axis tactile sensors are mounted on fingertips of two robotic fingers to perform object handling tasks. We have developed a control system consist of finger and sensor controllers. A control algorithm was designed in the robotic fingers system which applying normal and shearing forces obtained by the tactile sensors to control the movements of fingers during grasping tasks. The performance of this system was evaluated in object handling experiment using a wood block as an object. Experimental results shows that the robotic fingers managed to grasp the object within optimum grasp pressure and performed handling tasks without causing damage to the object or the sensor elements. The optical three-axis tactile sensor revealed good performance to use in robotic finger system.

In this chapter, we have shown that the robotic finger system equipped with the hemispherical shaped tactile sensors is suited for refining grips on object surface. Furthermore, the applied control algorithms are capable of preventing the probability of damage to the sensors and the object during robust grasping tasks. It is anticipated that using this novel optical three-axis tactile sensor in robotic grippers, with further improvement on hardware structure and image processing technique, will help advance the evolution of real-time object manipulation based on tactile sensing in robotic systems.

9. Acknowledgement

8. References

Hanafiah, Y., Ohka, M., Kobayashi, H., Takata, J., Yamano M. & Nasu Y. (2006). Contribution to the development of contact interaction-based humanoid robot navigation system: Application of an optical three-axis tactile sensor, *3rd Int. Conf. on Autonomous Robot and Agents (ICARA06)*, pp. 63-68

Hanafiah Y., Ohka, M., Suzuki, H., Morisawa N. & Takata, J. (2007). Sensing performance of an optical three-axis tactile sensor system with application in multi-fingered humanoid robot arm, *World Congress on Engineering & Computer Science (WCECS07), Int. Conf. on Intelligent Automation and Robotics (ICIAR07)*, pp. 504-509

Hanafiah Y., Ohka, M., Takata, J., Nasu Y. & Yamano, M. (2008). Low force control scheme for object hardness distinction in robot manipulation based on tactile sensing, *IEEE International Conference on Robotics and Automation (ICRA2008)*, pp. 3443-3448

Kerpa, O., Weiss, K. & Worn, H. (2003). Development of a flexible tactile sensor system for a humanoid robot, *Intl. Conf. on Intelligent Robots and Systems IROS2003*, CDR

Kuniyoshi, Y., Ohmura, Y. & Terada, K. (2004). Embodied basis of invariant features in execution and perception of whole-body dynamic actions – knacks and focuses of roll-and-rise motion, *Journal Robotics and Autonomous Systems*, Vol. 48, pp. 189-201

Lee, M. H. & Nicholls, H. R. (1999). Tactile sensing for mechatronics – a state of the art survey, *Journal Mechatronics*, Vol. 9, pp. 1-31

Natale, L. & Torres-Jara, E. (2006). A sensitive approach to grasping, *Proceeding 6th International Conference on Epigenetic Robotics*, CDR

Nicholls, H. R. (1990). Tactile sensing using an optical transduction method, *Traditional and Non-Traditional Robot Sensors (Edited by T. C. Henderson)*, Springer-Verlag, pp. 83-99

Ohka, M., Mitsuya, Y. & Matsunaga Y. (2004). Sensing characteristics of an optical three-axis tactile sensor under combined loading, *Robotica*, vol.22, pp. 213-221

Ohka, M., Kobayashi, H. & Mitsuya, Y. (2006). Sensing precision of an optical three-axis tactile sensor for a robotic finger, *15th IEEE International Symposium on Robot and Human Interaction Communication (RO-MAN2006)*, pp. 220-225

Ohmura, Y., Kuniyoshi, Y. & Nagakubo, A. (2006). Conformable and scalable tactile sensor skin for curved surfaces, *Proceeding International Conference on Robotics and Automation (ICRA2006)*, pp. 1348-1353

Ohmura, Y. & Kuniyoshi, Y. (2007). Humanoid robot which can lift a 30kg box by whole body contact and tactile feedback, *2007 IEEE/RSJ International Conference on Intelligent Robots and Systems (IROS2007)*, pp. 1136-1141

Omata, S., Murayama, Y. & Constantinou, C.E. (2004). Real time robotic tactile sensor system for determination of the physical properties of biomaterials, *Journal of Sensors and Actuators A*, Vol. 112, pp. 278-285

Schmidt, P. A., Mael, E. & Wurtz, R. P. (2006). A sensor for dynamic tactile information with applications in human-robot interaction and object exploration, *Journal Robotics & Autonomous Systems*, Vol. 54, Issue 12, Dec. 2006, pp. 1005-1014

Takata, J. (2006). Object recognition and manipulation using a robotic hand equipped with optical three-axis tactile sensors, *Master Thesis*, Department of Electro-Mechanical Engineering, Graduate School of Engineering, Nagoya University, Japan

Umetani Y. & Yoshida K. (1989). Resolved Motion Rate Control of Space Manipulators with Generalized Jacobian Matrix, *IEEE Transactions on Robotics and Automation*, Vol. 5(3), pp. 303-314

Sensors: Focus on Tactile Force and Stress Sensors

Edited by Jose Gerardo Rocha and Senentxu Lanceros-Mendez

This book describes some devices that are commonly identified as tactile or force sensors. This is achieved with different degrees of detail, in a unique and actual resource, through the description of different approaches to this type of sensors. Understanding the design and the working principles of the sensors described here requires a multidisciplinary background of electrical engineering, mechanical engineering, physics, biology, etc. An attempt has been made to place side by side the most pertinent information in order to reach a more productive reading not only for professionals dedicated to the design of tactile sensors, but also for all other sensor users, as for example, in the field of robotics. The latest technologies presented in this book are more focused on information readout and processing: as new materials, micro and sub-micro sensors are available, wireless transmission and processing of the sensorial information, as well as some innovative methodologies for obtaining and interpreting tactile information are also strongly evolving.

How to reference

In order to correctly reference this scholarly work, feel free to copy and paste the following:

Hanafiah Yussof, Jumpei Takata and Masahiro Ohka (2008). Measurement Principles of Optical Three-Axis Tactile Sensor and its Application to Robotic Fingers System, Sensors: Focus on Tactile Force and Stress Sensors, Jose Gerardo Rocha and Senentxu Lanceros-Mendez (Ed.), ISBN: 978-953-7619-31-2, InTech, Available from: http://www.intechopen.com/books/sensors-focus-on-tactile-force-and-stress-sensors/measurement_principles_of_optical_three-axis_tactile_sensor_and_its_application_to_robotic_fingers_s

INTECH

open science | open minds